

Comparison of Crossflow Turbine Performance through Nozzle Position Variations Using ANSYS Simulation

Corvis L Rantererung^{a,*}, Atus Buku^a

^a Mechanical Engineering Department, Paulus Christian University of Indonesia, South Sulawesi, Indonesia

Corresponding author: *corvisrante@yahoo.com

Abstract—The performance comparison of Crossflow turbines is greatly influenced by the position of the nozzle in the conversion of water energy into mechanical energy that occurs through the blades, runners, and shafts of Crossflow turbines. The study aims to directly examine the visualization of water fluid dynamics across the turbine runner blade and enhance the performance of the Crossflow turbine by varying the nozzle position. This study intends to investigate the impact of water flow dynamics and emission on the performance of Crossflow turbines with a combined horizontal-vertical nozzle position, specifically focusing on the magnitude of the number of turbine blades driven and the size of the runner blade area. The objective of investigating nozzle position variations in Crossflow turbines is to determine the specific nozzle position at which the turbine blade may efficiently extract maximum energy from the water flow, hence optimizing turbine performance. The research method using models made using CAD software is AutoCAD by exporting to IGES or IGS format to be compatible with ANSYS. The simulation of this research is with post-processing. There are three, namely making animations, making contours, and taking data to compare cross-turbine performance using variations in nozzle position. Crossflow turbine performance with horizontal nozzle position torque and turbine power is lower, and there is an increase in a vertical position. Then, the horizontal and vertical nozzle position is very good because the nozzle is more effective with maximum turbine performance, namely 13.811-watt turbine power 1,099 turbine torque at 120 rpm.

Keywords—Crossflow turbine; turbine performance; nozzle position variation; ANSYS simulation.

Manuscript received 17 May. 2023; revised 21 Aug. 2023; accepted 18 Oct. 2023. Date of publication 31 Dec. 2023.
IJASEIT is licensed under a Creative Commons Attribution-Share Alike 4.0 International License.



I. INTRODUCTION

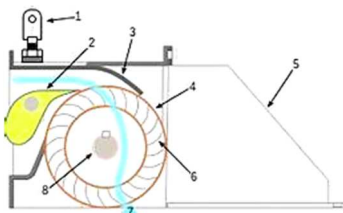
The most famous Crossflow water turbine in rural communities that harnesses the potential water energy as a fundamental energy source available naturally in nature is very environmentally friendly if it can be converted to mechanical forms of energy, electrical energy, and other energy. Improving the quality of life and human civilization is very proper if it uses water energy technically, economically, environmentally friendly, and sustainably [1]–[9]. Water energy in rivers and irrigation canals in rural areas can be used as an energy source to drive micro hydropower plants to serve the community sustainably and economically. The advantages are that the power output is adaptable to conditions and needs, reliable, durable to technology, has low operational costs, and has less environmental impact. Micro hydropower plants can utilize water flow energy freely with a slight discharge, and low head can use Crossflow turbines because of accessible technology, cheap with simple production [3], [10]–[15].

Crossflow turbines have been developed in depth with various methods. The performance of Crossflow turbines is significantly affected by the blade count and the turbine radius ratio [16], [17]. Crossflow turbines are very good to use at low waterfall heights and small water discharge capacities, with straightforward construction, are easy to manufacture, only using local materials and according to the needs in remote areas [11], [18]–[20]. Performance in Crossflow turbines is highly dependent on nozzle position, number of nozzles, geometric shape of turbine blades, fluid flow dynamics, head, water discharge, and energy loss from fluid flow on turbine blades [1], [2], [7], [21]–[28]. The absorption and utilization of water energy through the surface of the water turbine blades is inclined by the dynamic pattern of fluid flow and the concentration of water energy transfer on the surface of the runner blades for mechanical energy conversion as a turbine drive [4]–[6], [9], [29]–[36]. As per the real conditions in the field, Crossflow turbines are already widely used as initial movers in micro hydropower plants in many remote and underdeveloped rural areas [3], [10], [14], [37]–[40].

The most important thing to note in the installation of Crossflow turbine utilization is the emission of inlet water through the nozzle, the component gap between the casing and the runner usually leaks water flow, or there is an excess flow in the penstock pipeline that directs the flow of water into the turbine [21]–[28]. Proper positioning of the turbine blades increases the torque and power of the water turbine as a good main performance. Radial impulse turbines with crossflow turbine types are widely used in various micro hydropower plants in remote areas with small discharges at low water head levels [6], [41], [42]. This Crossflow turbine is very interesting to develop and pursue continuously to improve its performance compared to other water turbines [43]–[46]. It has been popular in the community that Crossflow impulse turbines are straightforward and compact in construction. The main component is two parallel disk circles and a series of turbine blades combined to form a simple turbine runner [47]–[52].

In Crossflow water turbines, there is a dynamic flow of water across the surface of the runner blades with two stages, namely through the first stage, the water jets out of the nozzle and then enters the front edge of the blade to the center of the turbine across the shaft. In the second stage, a jet or jet of water flows from the inside to the outer edge, passing to the next lower blade runner. Then, water radiates from the turbine and is discharged [53]–[55]. The phenomenon of water flowing across the turbine runner twice causes this type of turbine to be given the name Crossflow turbine, and it can convert the kinetic energy of the water jet from the nozzle twice into turbine mechanical energy [49]–[52]. The turbine nozzle is one of the main components of the turbine that functions as a guide and produces water jets to the runner blades of the water turbine [1], [2], [7], [16], [56]. The turbine runner blade component helps receive water beam collisions and then absorb water emission energy from the nozzle when crossing the surface of the water turbine runner blade. Then, the kinetic energy of water absorbed on the surface of the runner blade is passed onto the turbine shaft, which causes rotational motion in the runner [37]–[40], [53]–[55].

The crossflow turbine still has low performance compared to other types of water turbines. So, based on theory, experiment, and practices, information was obtained that the type of Crossflow turbine with a single nozzle at this time, many parts of the turbine blades that the water beam from the turbine nozzle has not touched. Hence, the torque and power of the turbine are still low. The type of Crossflow turbine with a single nozzle in a horizontal position is shown in Figure 1.



1. Air Venting Valve, 2. Distributor, 3. Casing of Turbine, 4. Runner of Turbine, 5. Removable Casing, 6. Blades of Turbine, 7. Flow of Water, 8. Shaft of Turbine

Fig. 1 Water fluid flow model on the Cross turbine [57]

Under the discharge capacity of water entering the turbine blades, crossflow can be calculated [6], [41], [42] using equation (1) as follows:

$$Q = \frac{\sqrt{2 \cdot A \cdot g \cdot h}}{t} = V/t \left(\frac{m^3}{s} \right) \quad (1)$$

Notes:

A= Nozzle cross-sectional area (m²).

g = Earth's gravitational acceleration constant (m/s²).

h = surface head level height air (m)

V= water volume (m³).

t = time (s).

To find out the waterpower needed by a plant by utilizing water energy is greatly affected by the magnitude of the flow capacity and the height of the waterfall [16], [56], calculated according to equation (2) below:

$$P_{input} = Q * h * \rho * g \quad (\text{Watt}) \quad (2)$$

The symbol in equation (2) with the description that P_{Input} = input power from water to turbine (Watt), Q = water flow rate (m³/s), h = height of falling water or head (m), ρ = density of water (kg / m³), g = acceleration of gravity (m/s²). The high level or head of water directed into the nozzle converts energy of water pressure into water kinetic, which causes water jets to drive turbine blades and rotate turbine shaft components. The calculation of torque capacity and power generated in Crossflow turbines results from converting water energy absorbed by turbine blades into mechanical energy as the primary mover of the rotating turbine shaft [58], [59]. The calculation follows equation (3) below.

Torque:

$$\tau = F \cdot r \quad (n.m) \quad (3)$$

Turbine Power:

$$P_{Output} = \tau \omega \quad (\text{Watt}) \quad (4)$$

The purpose of the study is to observe the visualization directly of the dynamics of water fluid across the turbine runner blade and improve the Crossflow turbine performance with variations in nozzle position. The magnitude of the number of turbine blades driven or the size of the runner blade area is crossed by the dynamics of water flow emission and its effect on the performance of Crossflow turbines with a combined horizontal-vertical nozzle position. Nozzle position variations in Crossflow turbines also aim to see directly at which nozzle position the turbine blade can absorb as much energy from the water flow beam as possible to improve turbine performance optimally. Crossflow turbines' high and low performance in turbine torque and power is convincingly affected by the pattern or dynamics of fluid flow across the angle that moves the turbine blades that receive and absorb water energy [29], [30], [45], [46], [31]–[36], [43], [44].

II. MATERIALS AND METHOD

The geometry used simulates transient water turbines (changes with time). Because the water turbine that we will simulate rotates around it, we have to make two-fluid models: the rotating area (rotating) and the stationary area (enclosure). Remember that what we are modeling is the fluid of this system, so there is no need to create a solid model. The

research model is a simulation using Ansys Software, and in the simulation, the dynamics of water fluid flow flowing across the runner blade of the Crossflow turbine. Crossflow turbines with nozzle position variations are turbines that include dual nozzles, with one positioned horizontally and one positioned vertically, and the option to combine both nozzles in a horizontal-vertical configuration, as illustrated in the schematic model in Fig. 1 as follows:

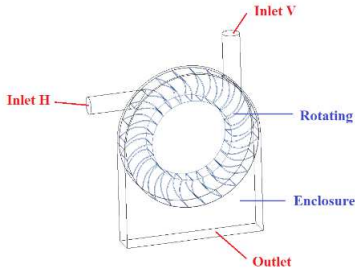


Fig. 2 Crossflow turbine model scheme with nozzle position variation

The model in Fig. 2 is created in CAD software, such as AutoCAD, by exporting to IGES or IGS format to be compatible with ANSYS.

A. Import Geometry to Ansys

First, open the ANSYS workbench and drag Fluid Flow into the workbench.

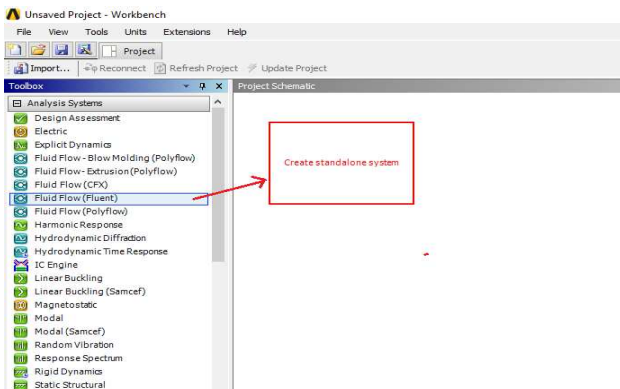


Fig. 3 Open ANSYS workbench and drag fluid flow

To quickly import geometry, right-click "geometry" and choose "import geometry." Then, browse and search the existing IGS file.

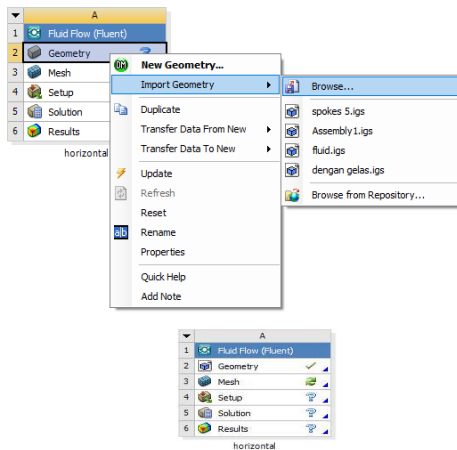


Fig. 4 Open ANSYS workbench and drag Fluid Flow (Fluent), Select Geometry

The tick on "geometry" indicates that geometry has successfully been imported.

B. Meshing

Double-click on "mesh" to open the meshing window. Click "geometry," then name each part by right-clicking and selecting "create named selection."

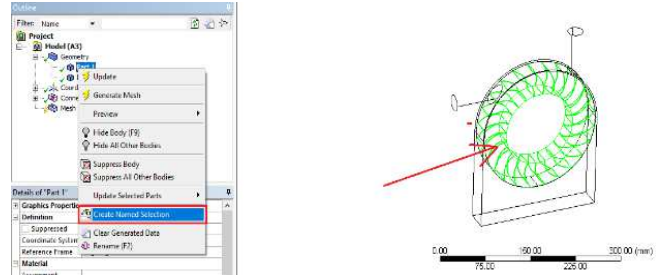


Fig. 5 Stage to open the Meshing window

Name it "rotating" for the inner geometry (part 1) and "enclosure" for the outside (part 2). Define inlets and outlets. Select selection to be face selection because we will select surfaces to define. Select the surface to be defined, then "create named selection" to name the surface.

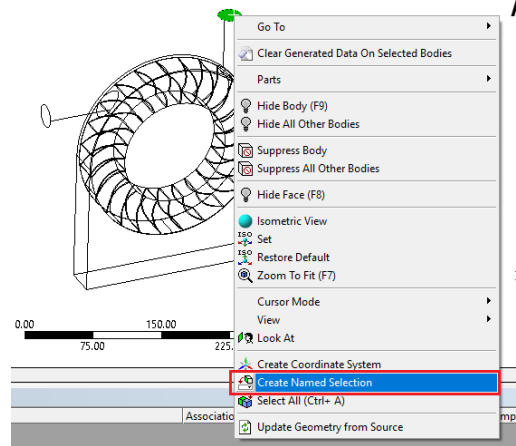


Fig. 6 Stage of "Create named selection" to name the surface

Name it according to the explanation in the geometry figure (topmost) consisting of inlet H, inlet V, and Outlet. After that, define the contact surface between the enclosure and the rotating by first hiding the outermost surface. Click all outermost surfaces (by holding down the Ctrl key), right-click, and select "Hide face":

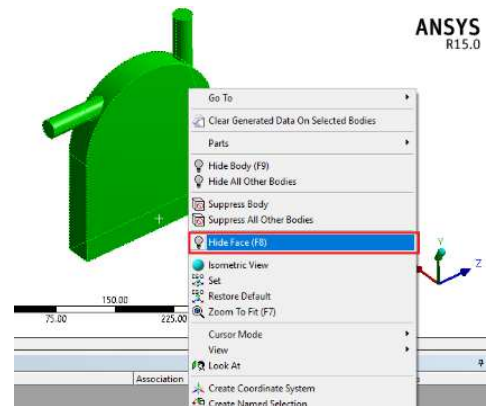


Fig. 7 Create a named selection and hide the face

Choose the 'outer' contact surface, i.e., the cylinder around the rotating. "Create named selection" and name it "outer int" (short for outer interface). Then, define the 'inner' contact surface by hiding the enclosure.

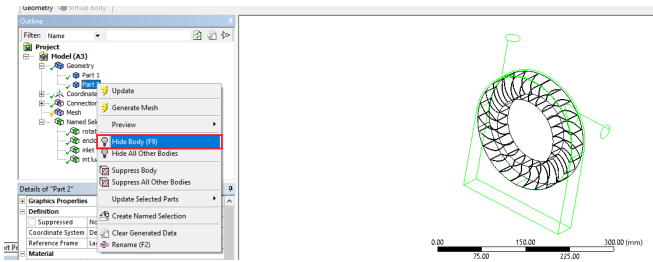


Fig. 8 Stage of creating Geometry and hiding body

Once only the rotating part is displayed, click all the outer surfaces to be named "inner int."

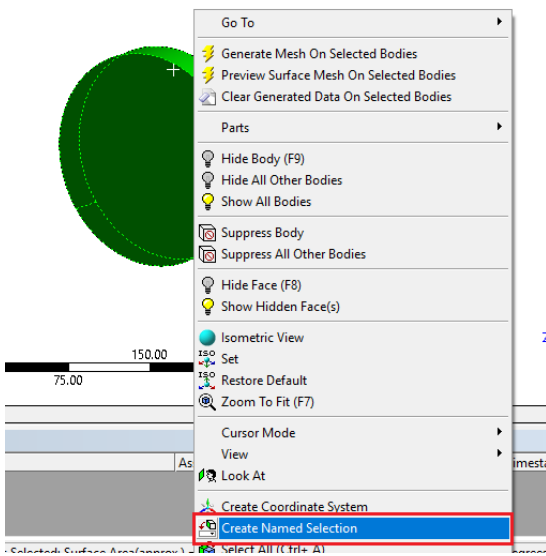


Fig. 9 Stage of creating named selection and rotating.

After defining all the parts, the next step is to define the contact between the enclosure and rotating with the settings below:

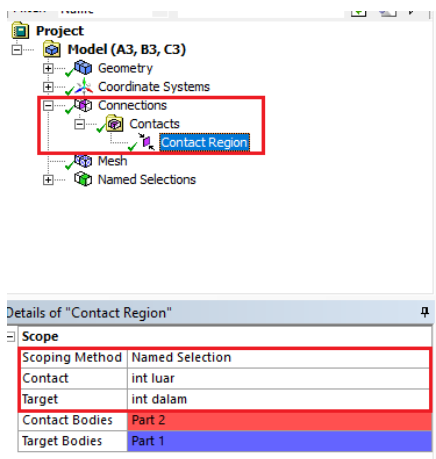


Fig. 10 Stage of defining enclosure contact region and contact bodies

The final step in the meshing process is defining the mesh itself. This case uses mesh with the following settings (explained below):

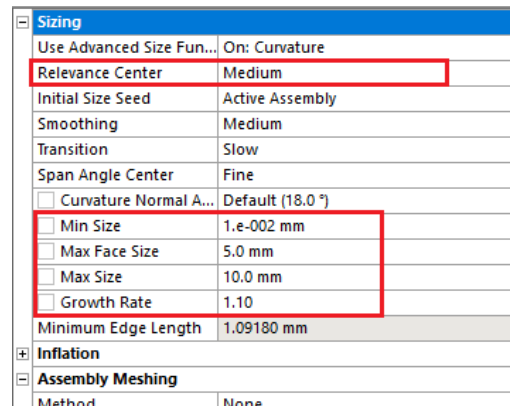


Fig. 11 Stage of Relevance Center

1) *Relevance center*: The fit of a mesh that is far from a feature. For example, there is a circle hole feature. A mesh with a high relevance center will adjust the mesh away from the circle.

2) *Min size, face size, max size*: We can determine the maximum and minimum size from the mesh. To set the overall mesh tenuous meeting.

3) *Growth rate*: The speed of mesh deployment. A high growth rate produces a mesh with an uneven density, while a low growth rate will produce a mesh with an even density.

The above values are primarily determined by the case and the operator's experience. However, the denser the mesh, the more accurate the results will be, and the flow pattern will be smoother. Mesh that is too dense results in computational processes that are too long and even makes solutions divergent (not convergent). Click "Update" to create the mesh. Right-click, then "show all body" and "show all face" to reshew the previously hidden geometry. The meshing process is complete.

C. Computing

Double-click the setup section. Select "parallel," then fill in the number of your processors. In the case of the computer, I use 4 processors, it may be possible to learn the maximum number of cores for other cores. The more processors are used, the faster the computing process, but other software runs slow. Click OK!

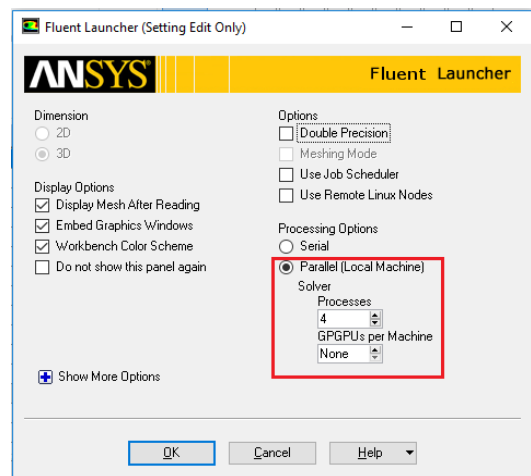


Fig. 12 Stage of display options, parallel (local machine)

Select the general settings as follows:

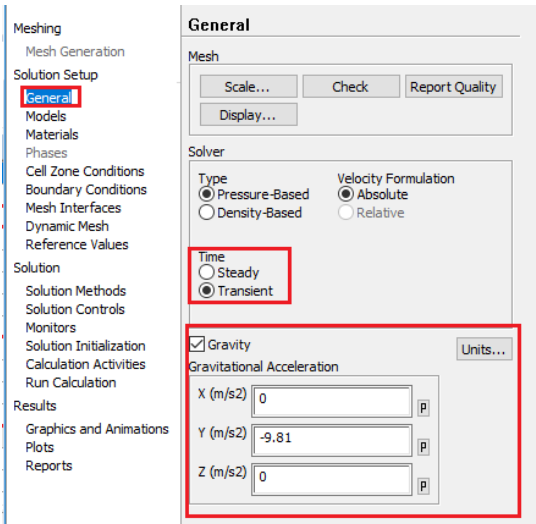


Fig. 13 Stage of Select level of general settings

Simulation is transient because there is a spin phenomenon in it. Define gravity in the direction according to the CAD model we created. Use the k-epsilon turbulent model (unless a previous journal already uses another model). The k-epsilon model was chosen because it is a conservative model for various cases and is known for its stability towards convergence.

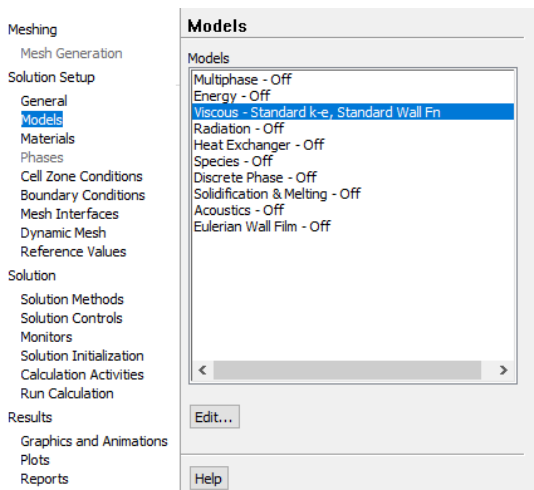


Fig. 14 Stage of selecting the general setting: Viscous Standard

Define a new water material by selecting material -> create/edit -> fluent database -> find water liquid.

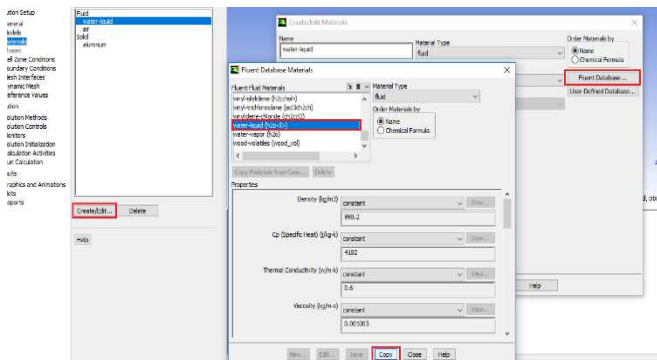


Fig. 15 Stage of select general setting; water liquid

Define an enclosure as water-liquid:

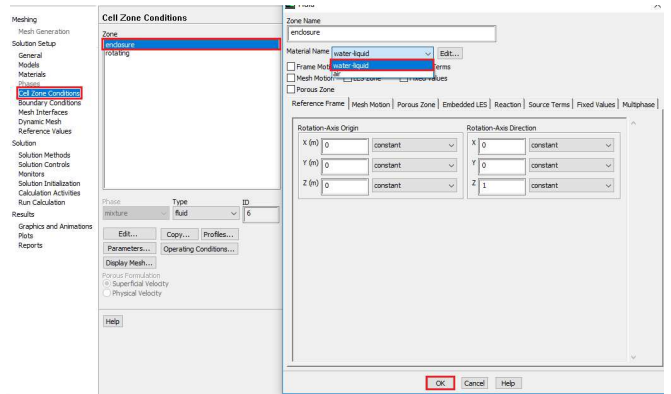


Fig. 16 Stage of select enclosure; water liquid

Define rotating as a rotating area with the following settings:

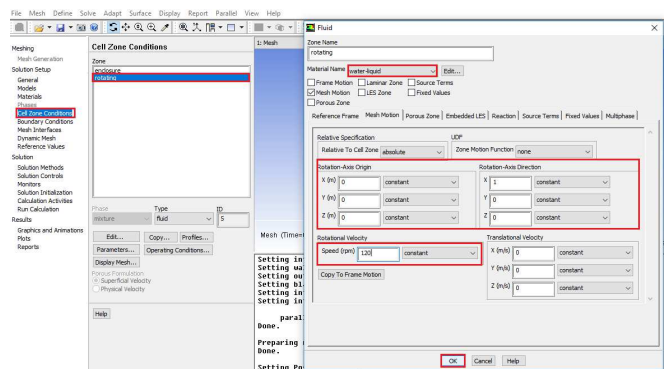


Fig. 17 Stage of select rotating; water liquid

It should be noted that the rotation axis origin and rotation axis direction must be adjusted to the CAD model that we made at the beginning. Try to make the CAD model we create have a center point in the middle of the rotating circle to make it easier to define the rotation axis origin. If your rotational velocity unit is not in RPM units, you can change it to define-> units. The boundary condition used is the head at the inlet, which is 3.5 m which is converted to pressure form with the equation. $P = \rho \cdot g \cdot H$ Choose one (inlet H or inlet V) as inlet pressure and another as the wall.

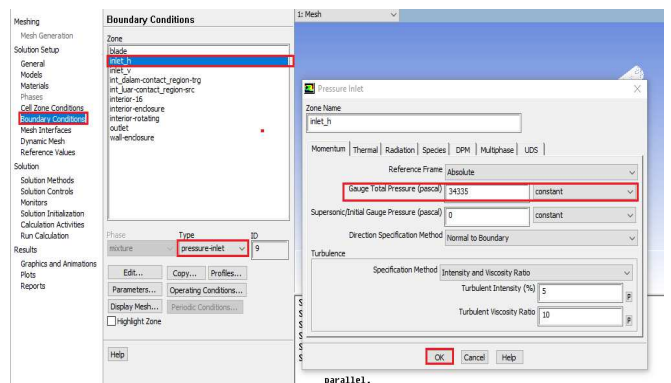


Fig. 18 Stage of selection either (inlet H or inlet V)

The next step is to define the interface. Since the existing interface cannot be edited directly, we must delete the existing interface first. Then, create a new interface, for example, with

the name "int", and define it according to the settings below. One of the crucial things is that we have to change the interface to "matching" to unify the enclosure flow and rotation. Click Create!

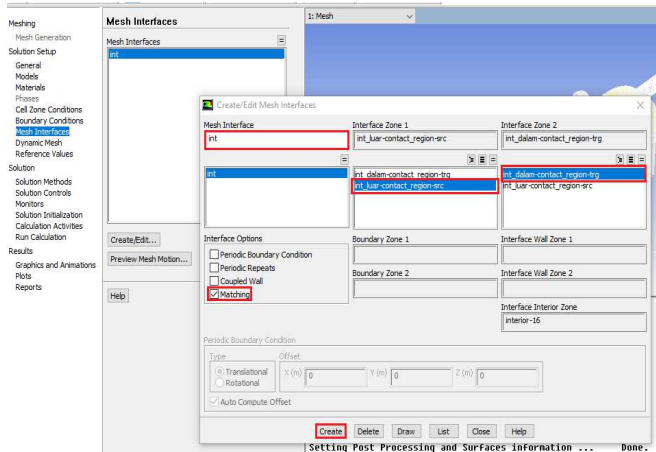


Fig. 19 Stage of select mesh interface.

The solution method, control, and monitors are not discussed in detail because they depend on operator experience and trial and error. Use the existing defaults if you are confused to edit them. Initialize each time you start a new simulation. Use a hybrid or standard initialization from one of the inlets we analyze. In calculation activities, setting "autosave every" with a low value will result in animations with smoother movements but will take up much memory and slow down the whole process. In this simulation, we use autosave every 1-time step to create animations and 5 for cases where torque data is needed only (no animation needed). Use the run calculation settings below:

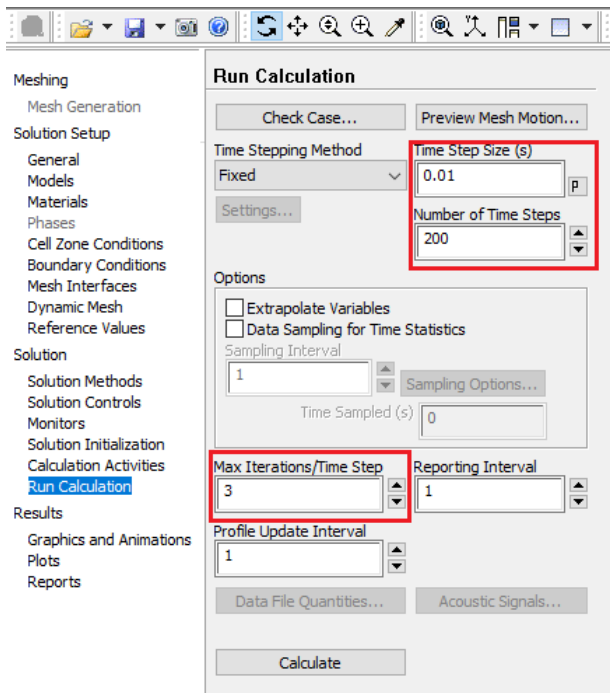


Fig. 20 Stage of Run Calculation

1) *Time steps*: This is the unit of time in seconds for each iteration. Like an animation, the smaller the time steps, the

smoother the movement. However, if it is too small, it will take a considerable number of steps (Number of time steps) to analyze at a specific time. The time analysis can be calculated by multiplying the time and number of time steps. Suppose Time steps = 0.01s, and the number of time steps = 200. Then, the time covered in the simulation is $0.01 * 200 = 2$ seconds.

2) *Autosave Every*: This value is the number of time steps when the frame is saved for later display in the animation. Suppose we input the value 5 in Autosave Every, while, we have a value of 0.01 s in time steps. Then, the image appearing in the animation is every $0.01 * 5 = 0.05$ second in the simulation. That is, if the simulation includes a simulation time of 2 seconds, then the total number of animation frames is $2 / 0.05 = 40$ frames (or images) to form the entire animation.

3) *Max iteration/time step*: The number of iterations each time step. Suppose we enter the value 3 in this parameter and 200 in the number of time steps. Then, the total iteration of this simulation is 300 times. The more Max iteration/time steps values, the more accurate the results, but the number of total iterations will be huge. Click Calculate to start the simulation and wait patiently. For new input, you only need to change the rpm value and reinitialize to reset the data and re-simulate with the new data.

D. Post Processing

The purpose of post-processing is threefold: making animations, making contours, and retrieving data.

1) *Data retrieval process*: Data taken from turbine simulations in torque and drag. Torque calculation can be calculated using the Calculators -> Function: Torque, Location: Blade, Axis: Global X. Calculate feature!

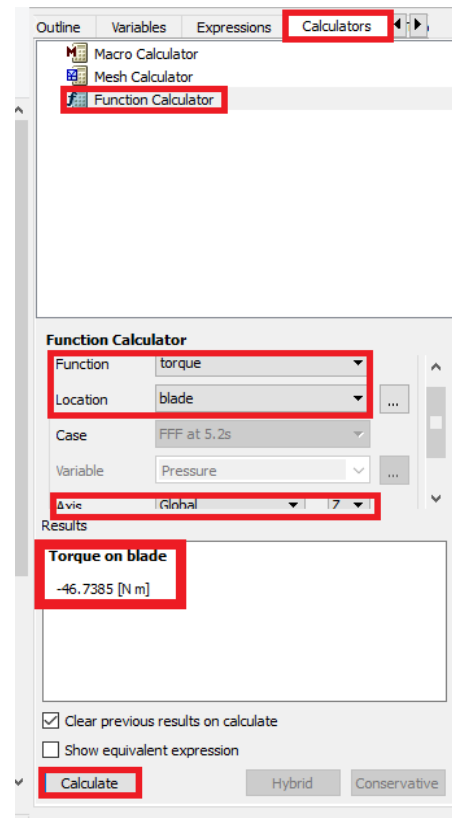


Fig. 21 Stage of Run Post-Processing

Remember that this simulation is transient; it changes with time. Therefore, the torque and drag values will change every second. To adjust the "position" of the time or angle of rotation, you can click on the "Time step selector". Double-click on the "time" you want.

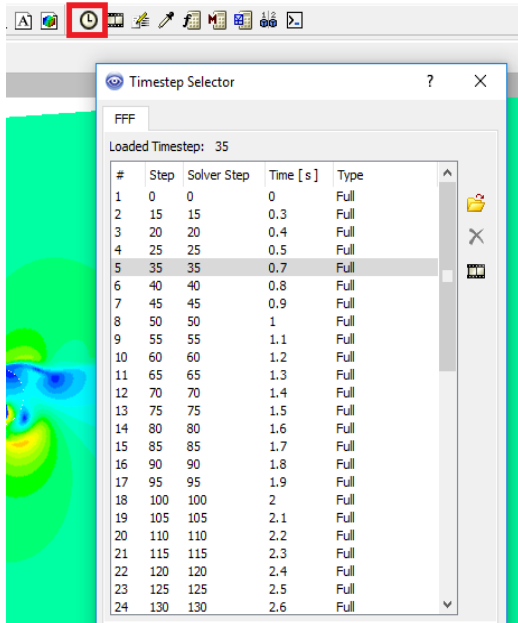


Fig. 22 The stage of sets the "position" of the time or angle of rotation, can be clicked on the "Time step selector"

2) *Creating a contour plot:* To create a contour plot, we first define the location where the plot is drawn by selecting the location -> plane menu. Select the plane's location as needed. Contours can be created by directly clicking on the shortcut "Contour". Use the settings below:

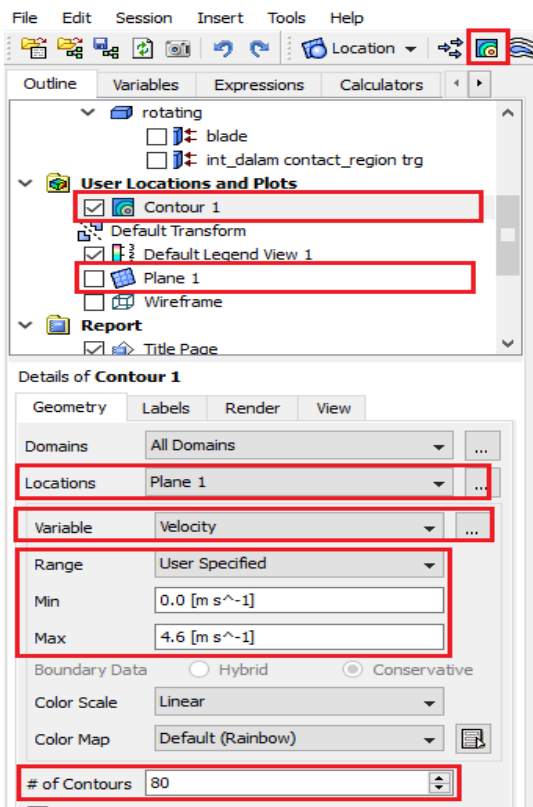


Fig. 23 Creating a contour plot

Choose a variable according to your needs, for example, velocity or pressure. The range -> user specified is used to maintain the consistency of simulation results. If the image is not intended to be simulated, it is recommended to use "local". # of higher contours will make the contour smoother, but too high a value can slow the extraction process in animation creation.

3) *Creating Animations:* Animation creation is done by returning to the shortcut "Timestep Selector", then selecting the block of all "time" and selecting the shortcut "Animate Timestep."

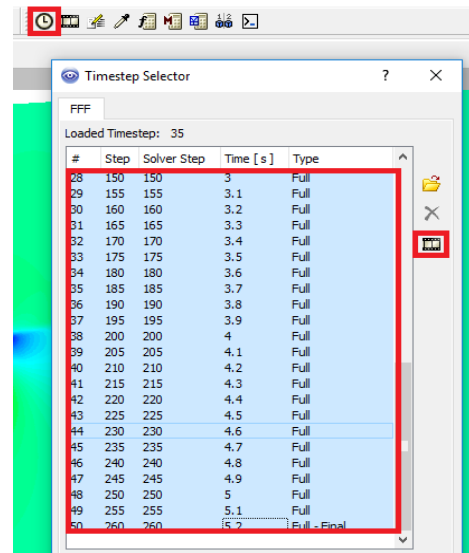


Fig. 24 Animation creation

Check "Save movie" and select the folder where you want to save the animation, then click the play icon to run the animation and save the animation.

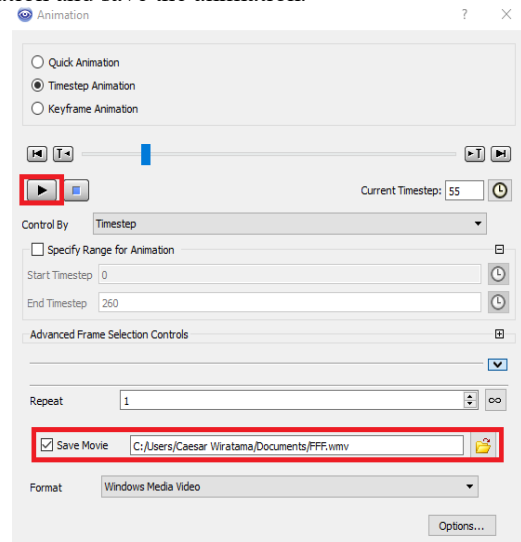


Fig. 25 Run animations while saving animations

III. RESULTS AND DISCUSSION

A. Simulating Crossflow Turbine Performance with Nozzle Position Variation

1) *Simulating Crossflow Turbine Performance with Nozzle Position Variation:* Based on the torque data

calculated from post-processing above, these data are compiled in Microsoft Excel by comparing them to rpm, and power can be calculated and tabled in Table 1.

2) *Animation of fluid dynamics in Crossflow turbine with horizontal nozzle position:* In Table 1, Figs. 26 and 27

illustrate Crossflow turbine performance with a horizontal nozzle position illustrating the spray of incoming water on the turbine runner blades. The animation of fluid flow dynamics is visible, which illustrates that in a Crossflow turbine with a horizontal nozzle, as shown in Fig. 28.

TABLE I
TURBINE CROSSFLOW PERFORMANCE SIMULATION RESULTS WITH NOZZLE POSITION VARIATIONS

No	Lap	Horizontal Nozzle Position		Nozzle Vertical Position		Horizontal and Vertical Nozzle Combined Position	
	rpm	Torque (nm)	Power (Watt)	Torque (nm)	Power (Watt)	Torque (nm)	Power (Watt)
1	120	0.806814	10.138723	0.915803	11.508319	1.0991	13.811697
2	140	0.542649	7.955649	0.627754	9.203354	0.7314	10.724335
3	150	0.461252	7.245329	0.527938	8.764069	0.6103	9.586962
4	160	0.363370	6.088322	0.408153	6.838669	0.5073	8.501065

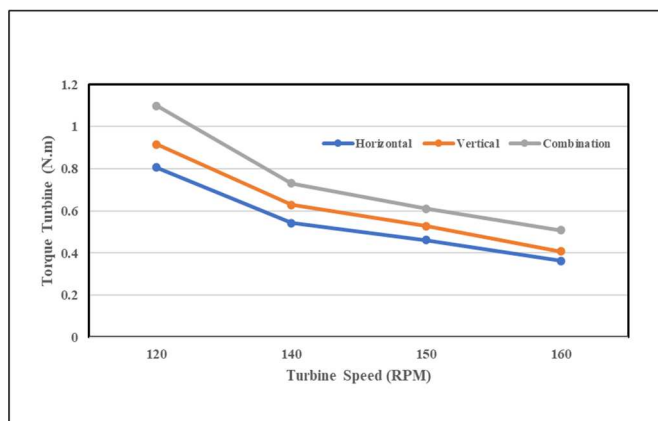


Fig. 26 Graph Turbin Torque Vs Turbine Speed

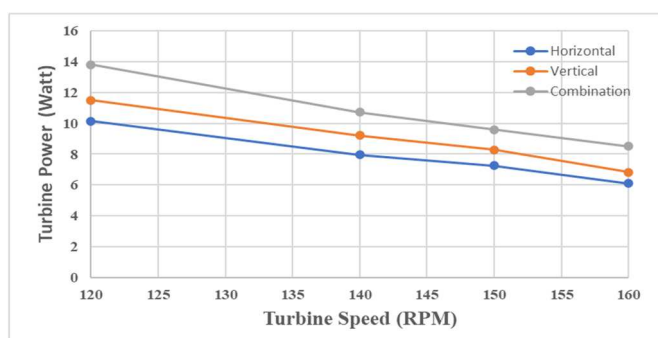


Fig. 27 Graph Turbine Power vs. Turbine Speed

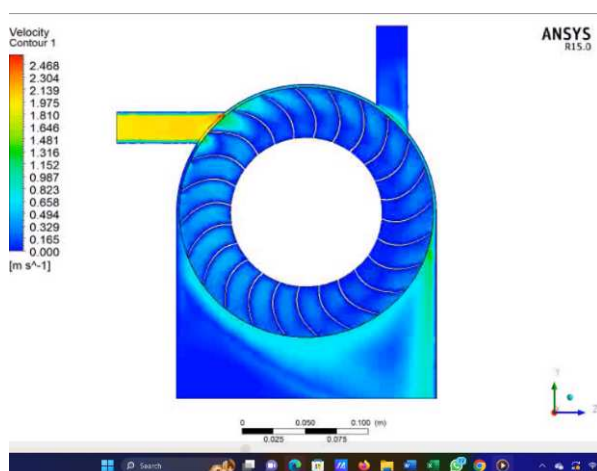


Fig. 28 Cross Flow Turbine Animation with Horizontal Position

Based on the animation results, the flow of water fluid is more stable through the runner blade chamber of the turbine. The *horizontal crossflow* nozzle radiates water to pound the driven turbine blades [3], [8]. The animation movement of water jets across the runner blade begins as a fluid flow moves the two-stage blade. According to the results of direct observations, the fluid dynamics generated by the horizontal nozzle propel the runner blade of the water turbine, allowing it to harness the energy of the water efficiently in a single stage [1], [2], [4]–[7], [9]. The optimal turbine power produced is lower in a Crossflow turbine using a horizontal nozzle position, which is 10.138 Watts, with a torque of 0.806 nm (Joule) because of fluid flow dynamics. The animation demonstrates the flow of the working fluid in a Crossflow turbine with a horizontally positioned nozzle. It illustrates that the working fluid, when emitted from the nozzle, imparts motion to the blades of the Crossflow turbine. Before reaching the blade chamber in the 2nd stage turbine, it results in the loss of hydraulic energy of the water jet and the change of water jet direction when entering the blade chamber of the second stage turbine, and conditions such as this significantly affect the reduction in turbine performance [3], [10], [14].

3) *Fluid animation on crossflow turbine with vertical nozzle position:* Table 1 and Figs. 26 27 above show the Crossflow turbine performance with a vertical nozzle position using a Crossflow turbine after operating or running stably and then visually observed the animation of the fluid flow Crossflow turbine with cross flow power with a nozzle position vertical began to increase by 11, 508 watts with a torque of 0.915 nm (Joule). The animated graphic demonstrates how a Crossflow turbine with a vertical nozzle emits and directs water into the turbine. Additionally, the animation showcases the fluid movement of water on a Crossflow turbine with a vertically positioned nozzle. Upon observing the animation image, it becomes evident that the animation of the fluid flow in the vertical nozzle crossflow turbine exhibits vertical radiation only. The water jet passes through the turbine blades in a crossflow configuration, exerting force on the blades in a single stage, allowing the blades to exclusively harness the energy from the water. The water jet entering the turbine solely impacts the blades, which causes the turbine performance with a vertical nozzle position to increase further, and the animated image can be seen in Fig. 29 as follows.

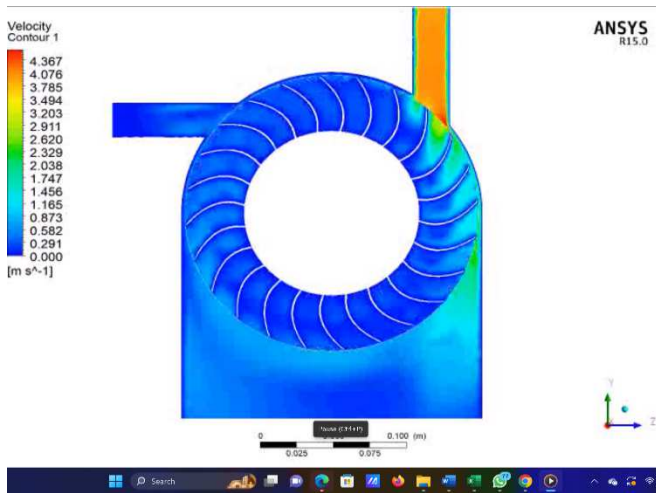


Fig. 29 Crossflow turbine animation with vertical position

4) *Animation of fluid flow on crossflow turbine with combined Horizontal and vertical nozzle positions:* The data from the research simulation described in Table 1 and Figs 26 and 27 above shows the crossflow turbine performance with a combination of horizontal and vertical nozzle positions is to receive water jets into the turbine from two stages, namely from the horizontal and vertical sides, this is so that more blades are crossed by water spray from the nozzle [11]–[13], [15]. The firsthand measurements unequivocally demonstrate the fluid flow dynamics that water jets generated, which originate from the nozzle. The drive for water turbine blades is achieved by a Crossflow pattern [17], [60]. The water beam emitted from the horizontal nozzle is guided by the water beam emitted from the vertical nozzle, resulting in enhanced absorption of water energy by the turbine blades leading to the increase of turbine's power and efficiency.

According to the animation pattern of fluid dynamics associated with the performance of the turbine cross nozzle, the combined horizontal-vertical nozzle position is substantial. Crossflow turbines have superior fluid flow dynamics, efficiently converting water energy into rotational motion by directing it onto the surface of the turbine blades. The graph in Fig. 9 clearly illustrates the positive correlation between turbine power and variations in water discharge. It is evident that when the flow rate increases, the turbine power also rises, highlighting the most significant difference [37]–[40]. The performance of Crossflow turbines with vertical horizontal combined nozzles has increased significantly, and the highest is 13,811-watt turbine power at 1,099 nm (Joule) of torque with 120 rpm rotation. Crossflow turbines with combined nozzles can produce greater turbine power and torque due to a more precise and effective fluid flow dynamics pattern in the direction of water jetting into the turbine runner blades [6], [41], [42]. The turbine runner absorbs more outstanding water energy blades to produce greater turbine shaft power, as illustrated in the animation in Fig. 30.

The fluid dynamics of the Crossflow turbine blades have a highly favorable impact on enhancing the performance of the turbine when equipped with the Horizontal-Vertical Combined Nozzle Position. It is essential to carefully evaluate the interaction between the turbine blade and the water jet that is released from the turbine nozzle. This can be achieved by adjusting the design of the turbine blade to align with the flow

that enters the blade area. The animation depicts the fluid flow dynamics that result in low turbine performance at low discharge. This occurs because the flow dynamics have sufficient time to fill the imperfections in the turbine blades and flow in a crossflow manner [11]–[13], [15].

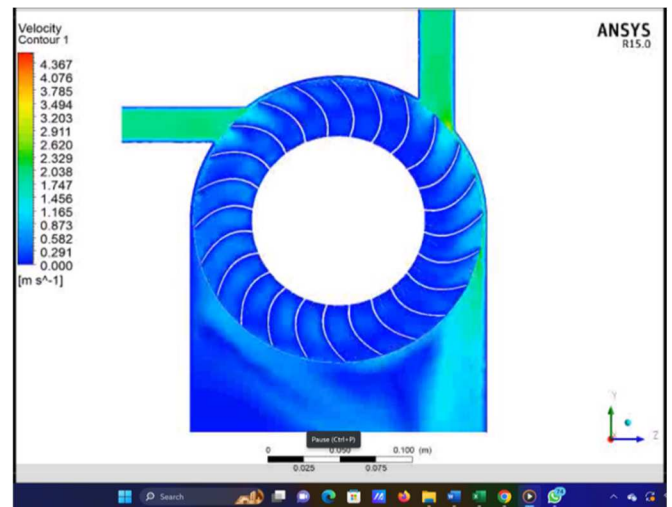


Fig. 30 Crossflow turbine animation with combined horizontal-vertical nozzle position

Nevertheless, when the velocity of the working fluid discharged from the nozzle is high, it prevents the working fluid from recirculating within the turbine blades. There is no crossflow movement from the uppermost blade level to the lower second blade level. By directly observing the image of the fluid flow pattern created by the water jet from the nozzle, it is evident that the fluid flow can reach multiple blades, resulting in the rotation of the water turbine. This rotation increases turbine power and torque, making it more efficient [11], [17]–[20], [60]. This shows that the more the speed of fluid flow increases, the more the inflow of turbine blades will tend to be turbulent. In Crossflow turbines using the horizontal nozzle position, the optimum turbine power produced is lower at 10.138 Watts, with a torque of 0.806 nm (Joule) because the water beam from the nozzle does not occur transverse flow. The turbine blade undergoes a single step of energy absorption, with only a limited number of blades propelled by water jets. The power output of the crossflow turbine rose by 11,508 Watts, and the torque increased by 0.915 nm (Joules) when the vertical nozzle position was adjusted. The Crossflow turbine exhibits a nozzle that is both vertical and horizontal in orientation. This design results in a substantial and maximum increase in turbine power, specifically 13,811 Watts at a torque of 1,099 nm (Joule) and a rotation speed of 120 RPM.

The velocity of lateral water flow, known as crossflow, significantly impacts the turbine's runner blades, leading to increased torque and power output. In a Crossflow turbine employing a combination of nozzle locations, the water jet emanating from the nozzle exerts a greater and more uniform force on the turbine blades, resulting in a twofold increase in the absorption of water energy by the blades. The crossflow turbine simulation results employ a configuration where the nozzle is positioned both horizontally and vertically. This arrangement allows the turbine blades to capture significant energy from the water flow efficiently, enhancing the

turbine's power output and maximum torque [53]–[55]. The combined Crossflow nozzle turbine is a turbine that operates twice. The efficient conversion and transfer of kinetic energy from water onto the turbine runner blade is effectively utilized to maximize the utilization of water energy sources as the primary driving force for a future power plant [53]–[55].

IV. CONCLUSION

The simulation settings we make produce power values in an order that approximates the results of experiments and simulations according to intuition. Then, based on the graph of power to rpm, a graph shows a trend of decreasing power to increasing rpm. Based on the graph of power to RPM, the overall performance at all rpm values, from highest to lowest, is combined inlet, vertical, and horizontal. The results of simulation and animation of fluid flow dynamics in a Crossflow turbine with a horizontal and vertical combined nozzle position preserve performance improvement due to water beam from the nozzle is able to cross the turbine runner and crossflow, more blades, drive the two-stage turbine runner blades, drive the turbine blades twice as many blades on the turbine runner. Achieve maximum turbine performance with a power of 13,811 Watts at a turbine torque of 1,099 with a rotation of 120 RPM. Crossflow turbines that use only horizontal or vertical nozzle positions show lower power performance, producing turbine torque.

REFERENCES

- [1] H. Olgun, "Investigation of the performance of a cross-flow turbine," *Int. J. energy Res.*, vol. 22, no. 11, pp. 953–964, 1998.
- [2] S. Chichkhede, V. Verma, V. K. Gaba, and S. Bhowmick, "A simulation based study of flow velocities across cross flow turbine at different nozzle openings," *Procedia Technol.*, vol. 25, pp. 974–981, 2016.
- [3] Z. Chen and Y.-D. Choi, "Influence of air supply on the performance and internal flow characteristics of a cross flow turbine," *Renew. Energy*, vol. 79, pp. 103–110, 2015.
- [4] M. Naseem, A. Saleem, and M. S. Naseem, "Investigation of blade design parameters for performance improvement of hydraulic cross flow turbine," *Ocean Eng.*, vol. 257, p. 111663, 2022.
- [5] G. Saini, R. P. Saini, and S. K. Singal, "Numerical investigations on performance improvement of cross flow hydro turbine having guide vane mechanism," *Energy Sources, Part A Recover. Util. Environ. Eff.*, vol. 44, no. 1, pp. 771–795, 2022.
- [6] N. Acharya, C.-G. Kim, B. Thapa, and Y.-H. Lee, "Numerical analysis and performance enhancement of a cross-flow hydro turbine," *Renew. energy*, vol. 80, pp. 819–826, 2015.
- [7] L. C. Rantererung, S. Soeparman, R. Soenoko, and S. Wahyudi, "Improvement Of performance crossflow turbine with dual nozzle," *ARPN J. Eng. Appl. Sci.*, vol. 13, no. 7, pp. 2364–2368, 2018.
- [8] I. A. Legonda, "An Investigation on the Flow Characteristics in the Cross-Flow Turbine-T15 300," *J. Power Energy Eng.*, vol. 04, no. 09, pp. 52–60, 2016, doi: 10.4236/jpee.2016.49005.
- [9] K. Kokubu, T. Kanemoto, S.-W. Son, and Y.-D. Choi, "Performance improvement of a micro eco cross-flow hydro turbine," *J. Adv. Mar. Eng. Technol.*, vol. 36, no. 7, pp. 902–909, 2012.
- [10] R. K. Ranjan, N. Alom, J. Singh, and B. K. Sarkar, "Performance investigations of cross flow hydro turbine with the variation of blade and nozzle entry arc angle," *Energy Convers. Manag.*, vol. 182, pp. 41–50, 2019.
- [11] Y. R. Pasalli and A. B. Rehiara, "Design planning of micro-hydro power plant in hink river," *Procedia Environ. Sci.*, vol. 20, pp. 55–63, 2014.
- [12] A. M. Durrani, O. Mujahid, and M. Uzair, "Micro hydro power plant using sewage water of Hayatabad Peshawar," in *2019 15th International Conference on Emerging Technologies (ICET)*, 2019, pp. 1–5.
- [13] A. Raza, D. Xu, M. S. Mian, and J. Ahmed, "A micro hydro power plant for distributed generation using municipal water waste with archimedes screw," in *INMIC*, 2013, pp. 66–71.
- [14] J. Haurissa, S. Wahyudi, Y. S. Irawan, and R. Soenoko, "The cross flow turbine behavior towards the turbine rotation quality, efficiency, and generated power," *J. Appl. Sci. Res.*, vol. 8, no. 1, pp. 448–453, 2012.
- [15] M. A. Khan and S. Badshah, "Research Article Design and Analysis of Cross Flow Turbine for Micro Hydro Power Application using Sewerage Water," *Res. J. Appl. Sci. Eng. Technol.*, vol. 8, no. 7, pp. 821–828, 2014.
- [16] B. Ben Amira, Z. Driss, S. Karray, and M. S. Abid, "PIV study of the down-pitched blade turbine hydrodynamic structure," in *Design and Modeling of Mechanical Systems: Proceedings of the Fifth International Conference Design and Modeling of Mechanical Systems, CMSM' 2013, Djerba, Tunisia, March 25-27, 2013*, 2013, pp. 237–244.
- [17] M. Sinagra, V. Sammartano, C. Aricò, A. Collura, and T. Tucciarelli, "Cross-Flow turbine design for variable operating conditions," *Procedia Eng.*, vol. 70, pp. 1539–1548, 2014.
- [18] A. A. Khan, A. Shahzad, I. Hayat, and M. S. Miah, "Recovery of flow conditions for optimum electricity generation through micro hydro turbines," *Renew. Energy*, vol. 96, pp. 940–948, 2016.
- [19] N. Zdankus, P. Punys, and T. Zdankus, "Conversion of lowland river flow kinetic energy," *Renew. Sustain. Energy Rev.*, vol. 38, pp. 121–130, 2014.
- [20] R. Abdullah and M. Islam, "Case study and model of micro hydro power plant using the kinetic energy of flowing water of Surma and Meghna rivers of Bangladesh," *Int. J. Sci. Technoledge*, vol. 2, no. 1, pp. 87–95, 2014.
- [21] H. Nautiyal, S. K. Singal, and A. Sharma, "Small hydropower for sustainable energy development in India," *Renew. Sustain. Energy Rev.*, vol. 15, no. 4, pp. 2021–2027, 2011.
- [22] S. Dudhani, A. K. Sinha, and S. S. Inamdar, "Assessment of small hydropower potential using remote sensing data for sustainable development in India," *Energy Policy*, vol. 34, no. 17, pp. 3195–3205, 2006.
- [23] D. Kumar and S. S. Katoch, "Small hydropower development in western Himalayas: Strategy for faster implementation," *Renew. Energy*, vol. 77, pp. 571–578, 2015.
- [24] M. Hossain *et al.*, "A state-of-the-art review of hydropower in Malaysia as renewable energy: Current status and future prospects," *Energy Strateg. Rev.*, vol. 22, pp. 426–437, 2018.
- [25] W. Uddin *et al.*, "Current and future prospects of small hydro power in Pakistan: A survey," *Energy Strateg. Rev.*, vol. 24, pp. 166–177, 2019.
- [26] K. S. Balkhair and K. U. Rahman, "Sustainable and economical small-scale and low-head hydropower generation: A promising alternative potential solution for energy generation at local and regional scale," *Appl. Energy*, vol. 188, pp. 378–391, 2017.
- [27] N. F. Yah, A. N. Oumer, and M. S. Idris, "Small scale hydro-power as a source of renewable energy in Malaysia: A review," *Renew. Sustain. Energy Rev.*, vol. 72, pp. 228–239, 2017.
- [28] M. K. Mishra, N. Khare, and A. B. Agrawal, "Small hydro power in India: Current status and future perspectives," *Renew. Sustain. energy Rev.*, vol. 51, pp. 101–115, 2015.
- [29] P. Gokhale *et al.*, "A review on micro hydropower in Indonesia," *Energy Procedia*, vol. 110, pp. 316–321, 2017.
- [30] C. P. Jawahar and P. A. Michael, "A review on turbines for micro hydro power plant," *Renew. Sustain. Energy Rev.*, vol. 72, pp. 882–887, 2017.
- [31] C. S. Kaunda, C. Z. Kimambo, and T. K. Nielsen, "A technical discussion on microhydropower technology and its turbines," *Renew. Sustain. Energy Rev.*, vol. 35, pp. 445–459, 2014.
- [32] A. H. Elbatran, O. B. Yaakob, Y. M. Ahmed, and H. M. Shabara, "Operation, performance and economic analysis of low head micro-hydropower turbines for rural and remote areas: A review," *Renew. Sustain. Energy Rev.*, vol. 43, pp. 40–50, 2015.
- [33] B. A. Nasir, "Design considerations of micro-hydro-electric power plant," *Energy procedia*, vol. 50, pp. 19–29, 2014.
- [34] S. Nababan, E. Muljadi, and F. Blaabjerg, "An overview of power topologies for micro-hydro turbines," in *2012 3rd IEEE International Symposium on Power Electronics for Distributed Generation Systems (PEDG)*, 2012, pp. 737–744.
- [35] M. Mohibullah, A. M. Radzi, and M. I. A. Hakim, "Basic design aspects of micro hydro power plant and its potential development in Malaysia," in *PECon 2004. Proceedings. National Power and Energy Conference, 2004.*, 2004, pp. 220–223.
- [36] A. A. Williams, "Pumps as turbines for low cost micro hydro power," *Renew. Energy*, vol. 9, no. 1–4, pp. 1227–1234, 1996.

- [37] J. M. R. Gorle, L. Chatellier, F. Pons, and M. Ba, "Modulated circulation control around the blades of a vertical axis hydrokinetic turbine for flow control and improved performance," *Renew. Sustain. Energy Rev.*, vol. 105, pp. 363–377, 2019.
- [38] M. Ali Kamran and S. Manzoor, "Effect of nozzle angle, turbine inlets and mass flow rate on the performance of a bladeless turbine," *Proc. Inst. Mech. Eng. Part A J. Power Energy*, vol. 234, no. 8, pp. 1101–1107, 2020.
- [39] X. Wu, H. Wu, L. Zuo, and B. Chen, "The effect of the blade number on a cross-flow hydrokinetic turbine," *IFAC-PapersOnLine*, vol. 55, no. 27, pp. 62–67, 2022.
- [40] N. C. V. Monintja, R. Soenoko, S. Wahyudi, and Y. S. Irawan, "The influence of flow steering angle on the performance of a cup-bladed kinetic turbine," *Int. J. Appl. Eng. Res.*, vol. 9, no. 20, pp. 7481–7489, 2014.
- [41] V. K. Yadav and S. K. Singal, "Performance analysis of cross-flow turbine: Variation in shaft diameter," in *Development of Water Resources in India*, 2017, pp. 487–497.
- [42] L. C. Rantererung, S. Soeparman, R. Soenoko, and S. Wahyudi, "Dual nozzle crossflow turbine as an electrical power generation," *ARPN J. Eng. Appl. Sci.*, vol. 11, no. 1, pp. 15–19, 2016.
- [43] A. H. Elbatran, O. B. Yaakob, Y. M. Ahmed, and M. R. Jalal, "Novel approach of bidirectional diffuser-augmented channels system for enhancing hydrokinetic power generation in channels," *Renew. Energy*, vol. 83, pp. 809–819, 2015.
- [44] K. W. Tan, B. Kirke, and M. Anyi, "Small-scale hydrokinetic turbines for remote community electrification," *Energy Sustain. Dev.*, vol. 63, pp. 41–50, 2021.
- [45] A. H. A. Elbatran, O. B. Yaakob, and Y. M. Ahmed, "Experimental Investigation of a Hydraulic Turbine for Hydrokinetic Power Generation in Irrigation/Rainfall Channels," *J. Mar. Sci. Appl.*, vol. 20, pp. 144–155, 2021.
- [46] R. Soenoko and S. Rispiningtati, "Prototype of a Twin Kinetic Turbine Performance as a Rural Electrical Power Generation," *J. Basic Appl. Sci. Res.*, vol. 1, no. 10, pp. 1686–1690, 2011.
- [47] A. O. Onokwai, H. I. Owamah, M. O. Ibiwoye, G. C. Ayuba, and O. A. Olayemi, "Application of response surface methodology (RSM) for the optimization of energy generation from Jebba hydro-power plant, Nigeria," *ISH J. Hydraul. Eng.*, vol. 28, no. 1, pp. 1–9, 2022.
- [48] K. A. Lempoy, R. Soenoko, S. Wahyudi, and M. A. Choiron, "Response Surface Methodology (RSM) Application toward the Performance of a Vertical Shaft Hinged Arc Blade Kinetic Turbine," *J. Eng. Sci. Technol.*, vol. 12, no. 8, pp. 2175–2186, 2017.
- [49] N. C. V. Monintja, R. Soenoko, S. Wahyudi, and Y. S. Irawan, "The vertical shaft kinetic turbine optimization using response surface methodology," *Int. J. Appl. Eng. Res.*, vol. 9, no. 21, pp. 8841–8856, 2014.
- [50] A. Tahir, M. Elgabaili, Z. Rajab, N. Buaossa, A. Khalil, and F. Mohamed, "Optimization of small wind turbine blades using improved blade element momentum theory," *Wind Eng.*, vol. 43, no. 3, pp. 299–310, 2019.
- [51] A. Abutunis, R. Hussein, and K. Chandrashekhara, "A neural network approach to enhance blade element momentum theory performance for horizontal axis hydrokinetic turbine application," *Renew. Energy*, vol. 136, pp. 1281–1293, 2019.
- [52] E. Tengs, P.-T. Storli, and M. Holst, "Optimization procedure for variable speed turbine design," *Eng. Appl. Comput. Fluid Mech.*, vol. 12, no. 1, pp. 652–661, 2018.
- [53] N. H. C. Pereira and J. E. Borges, "Study of the nozzle flow in a cross-flow turbine," *Int. J. Mech. Sci.*, vol. 38, no. 3, pp. 283–302, 1996.
- [54] O. Gusak, M. Cherkashenko, O. Potetenko, A. Hasiuk, and K. Rezvaya, "Improvement of operating processes of high-head tubular horizontal hydraulic turbines," in *Design, Simulation, Manufacturing: The Innovation Exchange*, Springer, 2021, pp. 126–136.
- [55] D. Sutikno, R. Soenoko, S. Soeparman, and S. Wahyudi, "Flow visualization of water jet passing through the empty space of cross-flow turbine runner," *Восточно-Европейский журнал передовых технологий*, no. 3 (8), pp. 36–42, 2019.
- [56] K. A. Lempoy, R. Soenoko, S. Wahyudi, and M. A. Choiron, "Movable blade vertical shaft kinetic turbine visual observation," *Восточно-Европейский журнал передовых технологий*, no. 2 (8), pp. 23–30, 2019.
- [57] Wikipedia, "Cross-flow turbine," 2023. https://en.wikipedia.org/wiki/Cross-flow_turbine.
- [58] M. Anyi and B. Kirke, "Evaluation of small axial flow hydrokinetic turbines for remote communities," *Energy Sustain. Dev.*, vol. 14, no. 2, pp. 110–116, 2010.
- [59] F. Bottiglione, S. De Pinto, and G. Mantriota, "Infinitely Variable Transmissions in neutral gear: Torque ratio and power re-circulation," *Mech. Mach. Theory*, vol. 74, pp. 285–298, 2014.
- [60] V. Sammartano, G. Morreale, M. Sinagra, and T. Tucciarelli, "Numerical and experimental investigation of a cross-flow water turbine," *J. Hydraul. Res.*, vol. 54, no. 3, pp. 321–331, 2016.